

Regular Article

Radon in Soil Gas and Ambient Dose Equivalent Rate Measurements in Yaoundé, Cameroon

Eric Gourda Hebsia¹, Oumar Bobbo Modibo^{1,2*}, Ayoba Ndimantchi¹,
Joseph Emmanuel Ndjana Nkoulou II², Eka Djatnika Nugraha³, Chutima Kranrod⁴,
Yasutaka Omori⁴, Masahiro Hosoda⁴, Saïdou^{1,2} and Shinji Tokonami⁴

¹Nuclear Physics Laboratory, Faculty of Science, University of Yaoundé I, P.O. Box 812, Yaoundé, Cameroon

²Research Centre for Nuclear Science and Technology, Institute of Geological and Mining Research, P.O. Box 4110, Yaoundé, Cameroon

³Research Centre for Technology of Radiation Safety and Metrology, The National Research and Innovation Agency of Indonesia (ORTN-BRIN), Jakarta 12440, Indonesia

⁴Institute of Radiation Emergency Medicine, Hiroasaki University, 66-1 Hon-cho, Hiroasaki-shi, Aomori 036-8564, Japan

Received 23 December, 2022; revised 2 August, 2023; accepted 12 June, 2024

This study measured radon (²²²Rn) concentrations in soil gas and ambient dose equivalent rates in various neighborhoods of Yaoundé, Cameroon. MARKUS 10 detector was used to measure radon in soil gas at 50 cm of depth. The ambient dose equivalent rate measurements were performed at the height of 1 m above ground, using a pocket survey meter (RadEye PRD-ER, Thermo Scientific). The results obtained from the radon concentration in soil gas measurements ranged from 8.4 to 50.7 kBq m⁻³ with a geometric mean of 25.4 kBq m⁻³. Ambient dose equivalent rates ranged from 0.02 to 0.11 µSv h⁻¹ with an average value of 0.05 µSv h⁻¹. These measurements were followed by calculating radon surface exhalation rates, and the annual outdoor external effective dose. Radon surface exhalation rates ranged from 41.5 to 250.5 mBq m⁻² s⁻¹ with an average value of 139.8 mBq m⁻² s⁻¹. The annual outdoor external effective dose varied between 0.07 and 0.39 mSv with an average value of 0.17 mSv. The correlation between radon concentration in soil gas and ambient dose equivalent rates was analyzed. A Pearson correlation coefficient $r = 0.81$ was obtained, indicating the strong correlation between them, and one can serve as the indicator of the other.

Key words: Radon, soil gas, ambient dose equivalent rate, exhalation rate, external effective dose.

1. Introduction

Humans are constantly exposed to radiation from natural and man-made radioactive sources that are unevenly distributed around the Earth. The natural component of

this radioactivity is due to radionuclides from the naturally occurring families of ²³⁸U, ²³⁵U, and ²³²Th, and from ⁴⁰K as well as cosmic radiation. According to ICRP Publ. 65⁽¹⁾, radon gas is the most important source (approximately 55%) of human internal radiation exposure.

Radon (²²²Rn) is a naturally occurring radioactive gas that comes from the decay of radium (²²⁶Ra) in the ²³⁸U decay chain present in the earth's crust. It is a colorless odorless, tasteless, inert gas that is generally present in all types of soil and rock, and its concentration varies

*Oumar Bobbo Modibo: Research Centre for Nuclear Science and Technology, Institute of Geological and Mining Research, P.O. Box 4110, Yaoundé, Cameroon
E-mail: bobbomodibo@gmail.com
https://doi.org/10.51083/radiatenviroinmed.13.2_52
Copyright © 2024 by Hiroasaki University. All rights reserved.

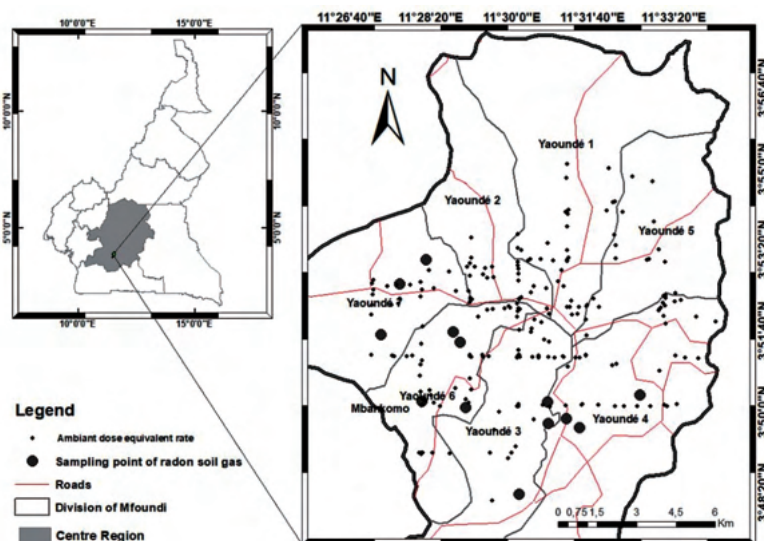


Fig. 1. Location of Yaoundé city with a highlight on the sampling points.

with the geological material and specific site²). Radon concentration level and radon risk will be increased with high uranium and radium content in soil³). So, radon is present everywhere on the earth's crust. The ^{222}Rn originates from geological substratum and diffuses through pore space in soil and rocks' fractures and along other weak zones as faults, and then it is transported by advection (described by Darcy's law) and diffusion (governed by Fick's law) through this space to exhale into the atmosphere^{4,5}).

Uranium and radium content of the soil, the type of the soil, the permeability of the soil, and physical parameters of the soil such as humidity, pressure, and temperature are factors that greatly affect the radon exhalation into the atmosphere and in indoor air. There are two main sources of radon in the indoor air: the soil and the water supply. Between the two sources, the soil is generally considered to be the higher source of radon in the indoor air. So, radon in the soil is the main cause of the radon problem. Radon has been classified as a lung carcinogen and is listed as the second risk factor for lung cancer, behind tobacco⁶). Extensive radon in soil gas measurements were being conducted worldwide for radiological risk assessment purpose⁷⁻¹³). Therefore, measuring the radon concentration in soil gas, its surface exhalation rate, and radiological parameters such as ambient dose equivalent rate is essential. Furthermore, the measurements of the ambient dose equivalent rate can serve as a good indicator for the estimation of radon concentration in soil gas. The research conducted by Tchorz-Trzeciakiewicz *et al.* in Poland showed that the ambient gamma dose rate can be used as a good indicator

of the geogenic radon potential¹⁴). Several studies in Germany, Switzerland, Hungary, Scotland, and Finland, used the gamma dose rate for predicting the radon flux on different rocks¹⁵).

The current work aimed to measure radon in soil gas and ambient dose equivalent rate in Yaoundé, Cameroon. From the concentrations of radon in soil gas, and the ambient dose equivalent rate measured, radon exhalation rates, and annual outdoor external effective dose were calculated, respectively. The correlation between the ambient dose equivalent rate and radon in soil gas was also analyzed.

2. Materials and methods

2.1. Geography and geology of the study area

The city of Yaoundé is located in the Region of Centre of Cameroon and it is the capital of the Country. It is located between $3^{\circ}52'00''$ North latitude and $11^{\circ}31'00''$ East longitude. Figure 1 presents the layout of the city of Yaoundé as well as the location of radon in soil gas sampling points. According to the Cameroon population census of 2005¹⁶), Yaoundé has a population of approximately 2.8 million inhabitants living in an area of 304 km^2 . Annual average precipitation and temperature in the city of Yaoundé are 1600 mm and $24\text{ }^{\circ}\text{C}$, respectively¹⁷). The climate of Yaoundé is equatorial type marked by two rainy seasons (March-June and September-November) and two dry seasons (December-February and July-August). Vegetation varies from degraded forest (south) to the post-forest savannah (north) and Mfoundi is the main river of the city of Yaoundé¹⁷). The geomorphology

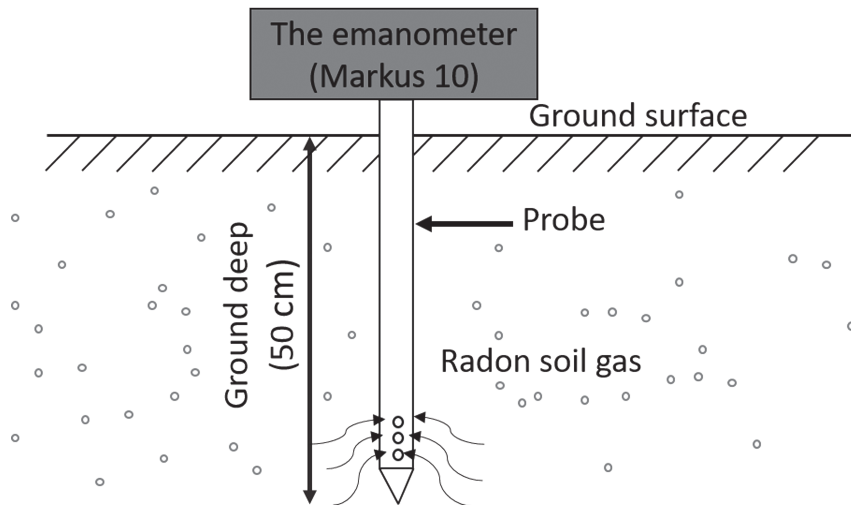


Fig. 2. Schematic diagram of the Markus 10.

is characterized by various landforms constituting mountainous massifs (> 800 m), plateaus (750 m), and swampy valleys (< 700 m).

Geologically, the Neoproterozoic basement of Yaoundé is composed of insoluble impervious and insoluble migmatites, schists, and gneisses which are transpierced by diachases and faults^{18, 19}. This basement gives permeability to the heterogeneous, anisotropic, and highly weathered formations and is responsible for the production of mostly well-drained Ferralitic soils. Mvondo *et al.* and Nzenti *et al.* reported that the most abundant outcrop along the beds of some rivers in Yaoundé city is metasedimentary rocks^{20, 21}. The Yaoundé bedrock is composed of fractured embrechites and is generally covered by alluvial hydromorphic clay and sand in the valleys and laterites (feralsols) on the hillsides²². The hydraulic investigations reported that the hydraulic conductivity values of Yaoundé varied between 8.17×10^{-7} and $2.26 \times 10^{-5} \text{ m s}^{-1}$ ²³.

2.2. Measurements of radon concentration in soil gas

The measurements of radon concentration in soil gas were performed using the MARKUS 10 detector, which is an electronic radon detector manufactured by Gammadata in Uppsala, Sweden. The MARKUS 10 radon detector is constituted with an air pump and a solid-state alpha detector which consists of a semiconductor material (Ortec Ultra Silicon) that converts alpha radiation directly to an electrical signal. The MARKUS 10 can differentiate immediately radon from thoron by the energy of the alpha particles released. The equipment is portable and battery-operated, and the measurement is fast. A stainless-steel probe supplied by Gammadata, immersed

in the soil, which was then connected to the MARKUS 10 detector with a water seal (special accessory for the purpose) was used to collect radon soil-gas samples of each measurement point. The probe was penetrated in the soil with a rotating handle or immersed with gentle strokes of a sledgehammer. For this study, the depth of the sampling points was set at 50 cm. The measurements were performed where the soil was generally free of rocks. The operation principle of the instrument is presented in Figure 2.

The MARKUS 10 operates by pumping out gas from the ground through a probe for 30 seconds. After the pumping phase, the Radon gas is driven and stored for 10 min in a measuring chamber, time during which it decays into its progeny (^{218}Po and ^{214}Po) through alpha radiation detected with an ultra-silicon surface barrier detector operating under a high electric field (~600 VDC)^{24, 25}. The detector pulses are amplified and filtered in an analyzer, which transmits only the pulses from the short-lived radon decay product, ^{218}Po . This eliminates the low background variations from ^{214}Po . The pulses are counted and converted by the device into volume concentrations in kBq m^{-3} . All these measurements were carried out during the daytime from 10 AM to 2 PM and in the absence of rainfall during the rainy season in May 2021. Period during which the average temperature and relative humidity were 24°C and 84%, respectively.

2.3. Calculation of radon surface exhalation rate

In the absence of disturbance, radon migration in the soil towards the atmosphere is ensured only by diffusion, described by the law of Fick. In the one-dimensional system, the diffusion flux density J of radon at the surface

of a porous medium assumed homogeneous and isotropic is defined by Fick's law expressed in Equation (1) ²⁶⁻²⁹:

$$J = -D \frac{dC_s}{dz}, \quad (1)$$

where D is the effective radon diffusion coefficient for natural soil ($4.62 \times 10^{-6} \text{ m}^2 \text{ s}^{-1}$)²⁹, and C_s is the radon concentration in the medium (Bq m^{-3}). C_s is the solution of the one-dimensional time-independent equation of radon diffusion through a porous medium described in Equation (2) ²⁶⁻²⁹:

$$D \frac{d^2 C_s}{dz^2} + \alpha - \lambda C_s = 0, \quad (2)$$

where α is the radon gas production rate in the medium's pore space ($\text{Bq m}^{-3} \text{ s}^{-1}$), λ is the radon decay constant (s^{-1}). Thus, the solution C_s of the Equation 2 is presented in Equation (3):

$$C_s = A e^{\sqrt{\frac{\lambda}{D}} z} + B e^{-\sqrt{\frac{\lambda}{D}} z} + \frac{\alpha}{\lambda} \quad (-\infty < z < 0). \quad (3)$$

When applying boundary conditions, when $z \rightarrow -\infty$, C_s should be finite, and when $z \rightarrow 0$, $C_s = 0$. It supposes the radon concentration at the soil surface from atmospheric apport is negligible. Thus, Equation 3 is substituted by Equation (4):

$$C_s = \frac{\alpha}{\lambda} \left(1 - e^{\sqrt{\frac{\lambda}{D}} z} \right). \quad (4)$$

From Equations (1) and (4), the radon diffusion flux density at the soil surface ($z = 0$) is expressed in Equation (5):

$$J_0 = \alpha \sqrt{D/\lambda} \quad (5)$$

Radon surface exhalation rate E ($\text{Bq m}^{-2} \text{ s}^{-1}$) at the soil surface is expressed using Equation (6)^{28, 29}:

$$E = \eta J_0, \quad (6)$$

where η is the soil porosity for natural soil (50%)²⁹. Thus, the Equation (6) can be substituted with the Equation (5) to express the radon surface exhalation rate in Equation (7):

$$E = \eta \alpha \sqrt{D/\lambda}. \quad (7)$$

Radon in soil gas concentration C_s remains in equilibrium in the medium, which means the radon decayed is replaced by the radon that is being produced. Thus, the radon production rate α is expressed in Equation (8)³⁰:

$$\alpha = \lambda C_s. \quad (8)$$

Finally, the radon surface exhalation rate on the soil surface is obtained using Equation (9):

$$E = \eta C_s \sqrt{\lambda D}. \quad (9)$$

2.4. Ambient dose equivalent rate measurements

Firstly, the outdoor ambient dose equivalent rate measurements were performed at a height of 1 m above ground, using a portable instrument (NucScout monitor manufactured by Sarad). It integrates a sensitivity NaI(Tl) scintillation detector with an integrated photo multiplier and high voltage supply³¹. The sampling interval for this study was adjusted to 12 min. Total activity is calculated by instrument software integrated from direct ²²⁶Ra detection, ²¹⁴Bi direct detection, ⁴⁰K detection, and ²⁰⁸Tl detection. The measurements with this instrument were carried out in the same places and at the same times during the measurement of radon concentrations in soil gas. Thus, thirteen points in Yaoundé were measured to study the correlation between the ambient dose equivalent rate and the concentration of radon in soil gas. Secondly, another ambient dose equivalent rate measurements were performed at 220 points in Yaoundé at the height of 1 m above ground, using a pocket survey meter (RadEye PRD-ER, Thermo Scientific). The instrument incorporates a high-sensitivity NaI(Tl) scintillation detector with a miniature photo-multiplier allowing the detection of very low radiation levels with an emphasis on gamma emissions below 400 keV. The results obtained from these measurements serve to assess the annual outdoor external effective dose.

2.5. Annual outdoor external effective dose assessment

The annual outdoor external effective dose was assessed using the formula expressed in Equation (10)³²:

$$E_{\text{ext}} = \bar{H} \times T_{\text{out}} \quad (10)$$

where \bar{H} is the arithmetic mean of ambient dose equivalent rate measured by the above-mentioned RadEye PRD-ER pocket survey meter, and T_{out} is the time passing outdoors during a year³².

3. Results and discussion

3.1. Radon concentration in soil gas

The results of radon measurements in soil gas in Yaoundé are given in Table 1. The lowest value of radon concentration in soil gas was recorded in the neighborhood of Nsam (8.4 kBq m^{-3}), while the highest value was recorded in the neighborhood of Ahala (50.7 kBq m^{-3}). The arithmetic mean and geometric mean of radon concentration in soil gas were 28.25 and 25.43 kBq m^{-3} , respectively. The highest radon concentration

Table 1. Radon concentration in soil gas, and radon surface exhalation rate

Statistical parameters	Radon concentration in soil (kBq m ⁻³)	Radon exhalation rate (mBq m ⁻² s ⁻¹)
Range	8.4-50.7	41.5-250.5
AM	28.3	139.8
GM	25.4	125.5
SD	12.3	60.7

AM: arithmetic mean, GM: geometric mean, SD: standard deviation

in soil gas observed in the neighborhood of Ahala could be explained by the presence of much higher relative humidity than at other measurement points. The measurement points at the neighborhoods of Nsam and Mvan show lowest levels of radon concentration in soil gas. In general, the variations of radon concentration in soil gas in the present study area may be due to porosity and density of soil, radium content and distribution, underlying bedrock and meteorological parameters of each measurement point (barometric pressure, rain, etc.), since that these parameters play important role in the release of radon in soil-gas³³.

The radon concentrations in soil gas obtained in this study were compared with those reported elsewhere. Petersell *et al.*⁷ reported radon concentrations in soil gas from Estonia in the range of 1-2112 kBq m⁻³, in Islamabad, Pakistan radon concentrations in soil gas ranged from 3 to 97 kBq m⁻³. Gondji *et al.* reported radon concentrations in soil gas ranging from 3.6 to 63.2 kBq m⁻³ at the Cobalt-Nickel Bearing Area of Lomié, in Eastern Cameroon³⁰. Al-bakhat *et al.* reported radon concentrations in soil gas between 0.87-16 kBq m⁻³ in Al-Tuwaitha Nuclear Site and the Surrounding Areas, Iraq²⁷. The radon concentration in soil gas from Franklin Mountain in El Paso, Texas in the United States of America ranged between 1.35-7.75 kBq m⁻³¹². The radon concentrations in soil gas at 1 m of depth in Northern Rajasthan, India ranged between 0.72-10.40 kBq m⁻³⁹. In Abeokuta, Southwest Nigeria, radon concentrations in soil gas studies reported a radon concentration in the range of 1-19.25 kBq m⁻³¹³. Around Castle Island, Co. Kerry in Ireland the radon concentrations in soil gas lie in the range of 10-1,433 kBq m⁻³⁸. Baiwa *et al.*³⁴ reported radon concentrations in soil gas from the Tusham ring complex of Haryana in the range of 42.80 to 71.50 kBq m⁻³. Radon concentrations in soil gas measured in the present investigation are in the range of the values reported in these cited studies except those in Estonia⁷, Islamabad district, Pakistan, Castle Island, Co. Kerry, Ireland⁸, and Tusham ring complex of Haryana⁹.

3.2. Radon surface exhalation rate

The radon surface exhalation rate was calculated from the measured values of radon concentrations in soil

gas. The calculated radon surface exhalation rates are presented in Table 1. Radon surface exhalation rates ranged from 41.5 to 250.5 mBq m⁻² s⁻¹ with a geometric mean value of 125.5 mBq m⁻² s⁻¹. It was seen from the results that, the radon surface exhalation rates varied significantly from one sampling point to another. This variation may be due to the differences in the large radium and uranium contents and porosity of each soil measurement point although it also depends on many other factors, such as permeability and density of soil, soil cover, texture, and grain size. The values of radon surface exhalation rates for the city of Yaoundé are higher than the reported worldwide mean of 16 mBq m⁻² s⁻¹, and those found in Kobe City (2 ± 2 - 30 ± 8 mBq m⁻² s⁻¹), in Gifu Prefecture (4.5 ± 0.3 mBq m⁻² s⁻¹), Japan^{35,37}. This could be explained by the geological and environmental factors of the study area and the methodology used for radon surface exhalation rate measurements. According to Hosoda *et al.*³⁶, the calculated radon surface exhalation rate values are usually higher than the directly measured values.

3.3 Ambient dose equivalent rate

The results of the ambient dose equivalent rates measurements obtained for this study are presented in Figure 3.

A total of 220 measurement points were recorded using a RadEye PRD-ER pocket survey meter. The ambient dose equivalent rate values varied from 0.02 to 0.11 µSv h⁻¹, with a mean value of 0.05 µSv h⁻¹. According to Gulan and Spasović³⁸ it is known that the outdoor ambient dose equivalent rate varies from place to place and also with meteorological parameters³⁹, relief, vegetation, and diversity soil composition. When compared with other studies, it can be stated that the range of results from the present study are lower than those in Celleno municipality in central Italy⁴⁰ which varies from 0.13 to 0.42 µSv h⁻¹ with an average of 0.22 µSv h⁻¹. However, the range values obtained in the present study are similar to the range values measured at Tuzla City, Bosnia and Herzegovina⁴¹. Furthermore, the mean value obtained in this study is higher than the mean value obtained at the Bunkyo Campus of Hirosaki University, Japan by Hosoda *et al.*⁴².

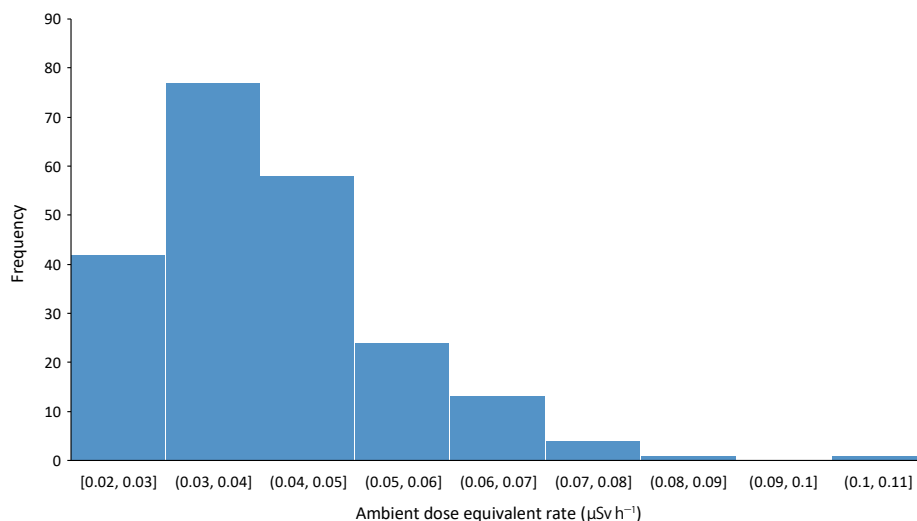


Fig. 3. Distribution of ambient dose equivalent rate in the city of Yaoundé.

3.4. Annual outdoor external effective dose

The annual outdoor external effective dose received by a member of the public living in the surrounding area was calculated from the results of the ambient dose equivalent rates measured using RadEye PRD-ER. It ranges from 0.07 mSv to 0.39 mSv with an average value of 0.17 mSv. These results indicate that the outdoor exposure of a member of the public to the external radiation in Yaoundé is not critical when compared to the values reported by Saïdou *et al.*, and Oumar Bobbo *et al.* in different regions of Cameroon. The authors found an average of annual outdoor external effective dose values of 0.7 mSv, and 1.2 mSv in Southern Adamawa, and Kitongo, respectively^{43,44}. These average values are higher than the ones obtained in the present study. However, the results of the present study are similar to those obtained by Koyang *et al.*, in the Far North Region of Cameroon⁴⁵.

3.5 Correlation between radon concentration in soil gas and ambient dose equivalent rate

The relationship between ambient dose equivalent rate and radon concentration in soil gas was studied. A Pearson correlation coefficient $r = 0.81$ was obtained and indicates ambient dose equivalent rate and radon concentration in soil gas in Yaoundé City are well correlated.

This correlation reveals a good dependence between radon concentration in soil gas and ambient dose equivalent rate. This is because radon decay products being gamma emitters contribute to external gamma radiation. These results indicate that it is possible to predict the radon in soil gas from the ambient dose equivalent rate⁹. The results obtained in the present study are in good agreement with those carried out in

other countries. Also, a positive correlation between radon concentration in soil gas and ambient dose equivalent rate was reported in Kumaon Himalaya, India, and Poland by Ramola *et al.* and Tchorz-Trzeciakiewicz *et al.*, respectively^{4,14}. Furthermore, the research conducted by Tchorz-Trzeciakiewicz *et al.* indicates that the ambient gamma dose rate can be a good indicator of the geogenic radon potential¹⁴.

4. Conclusion

Radon concentrations in soil gas measured in this study were found to vary between 8.4–50.7 kBq m⁻³, with a geometric mean of 25.4 kBq m⁻³ which is above the the global average range (0.4 to 40) kBq m⁻³. The ambient dose equivalent rate values varied from 0.02 to 0.11 μSv h⁻¹, with a mean value of 0.05 μSv h⁻¹. Radon surface exhalation rates ranged from 41.5 to 250.5 mBq m⁻² s⁻¹. The annual outdoor external effective dose varied between 0.07 and 0.39 mSv with an average value of 0.17 mSv. A strong correlation ($r = 0.81$), was obtained between radon concentration in soil gas and ambient dose equivalent rates. That indicates the ambient dose equivalent rate can be a good indicator of the radon concentrations in soil gas radon potential. Additional measurement points of ²²²Rn concentration in soil gas for the other major cities of Cameroon is required, to establish a complete database of the Country for radon risk mapping.

Acknowledgment

The International Atomic Energy Agency (IAEA) is thanked for its funding and its technical support through

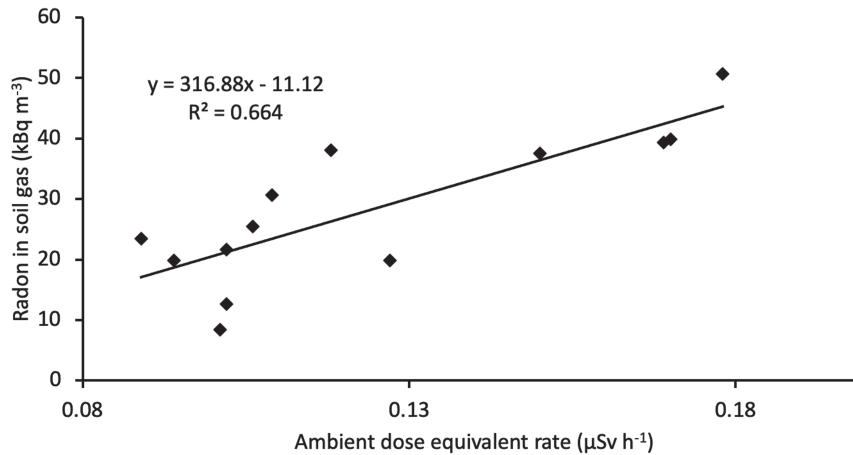


Fig. 4. Correlation between radon in soil gas and ambient dose equivalent rate.

the CMR9009 project. The Ministry of the Scientific Research and Innovation, of Cameroon is acknowledged for the support of the field work through the public investment budget 2021. This work was supported by ERAN Y-23-18.

Conflict of Interest

The authors declare that they have no conflict of interest.

References

- ICRP. Protection against Radon-222 at Home and Work, ICRP Publication 65. Ann ICRP 23(2). Oxford: Pergamon Press; 1993.
- Choubey VM, Bist KS, Saini NK, Ramola RC. Relation between soil-gas radon variation and different lithotectonic units, Garhwal Himalaya, India. *Appl Radiat Isot.* 1999;51(5):587–92.
- Ramola RC, Choubey VM, Negi MS, Prasad Y, Prasad G. Radon occurrence in soil–gas and groundwater around an active landslide. *Radiat Meas.* 2008;43(1):98–101.
- Ramola RC, Choubey VM, Prasad Y, Prasad G, Bartarya SK. Variation in radon concentration and terrestrial gamma radiation dose rates in relation to the lithology in southern part of Kumaon Himalaya, India. *Radiat Meas.* 2006;41(6):714–20.
- UNSCEAR. UNSCEAR 1988 Report to the General Assembly, with Scientific Annexes. Sources, Effects and Risks of Ionizing Radiation. New York: United Nations; 1988.
- WHO. Handbook on Indoor Radon: a Public Health Perspective. Geneva: World Health Organization; 2009.
- Petersell V, Täht-Kok K, Karimov M, Milvek H, Nirgi S, Raha M, *et al.* Radon in the soil air of Estonia. *J Environ Radioact.* 2017;166:235–41.
- Banrion MH, Elio J, Crowley QG. Using geogenic radon potential to assess radon priority area designation, a case study around Castleisland, Co. Kerry, Ireland. *J Environ Radioact.* 2022;251–252:106956.
- Duggal V, Rani A, Mehra R. Measurement of soil-gas radon in some areas of northern Rajasthan, India. *J Earth Syst Sci.* 2014;123(6):1241–7.
- Kumar S, Singh S, Bajwa BS, Sabharwal AD. In situ measurements of radon levels in water and soil and exhalation rate in areas of Malwa belt of Punjab (India). *Isot Environ Health Stud.* 2011;47(4):446–55.
- Kunovska B, Ivanova K, Stojanovska Z, Vuchkov D, Zaneva N. Measurements of radon concentration in soil gas of urban areas, Bulgaria. *Rom J Phys.* 2013;58(S):S172–9.
- López JA, Ornelas OD, Sajo-Bohus L, Rodriguez G, Chavarria I. Correlation between underground radon gas and dormant geological faults. *J Nuclear Phys Mater Sci Radiat Appl.* 2016;4(1):265–75.
- Samuel TD, Farai IP, Awelewa AS. Soil gas radon concentration measurement in estimating the geogenic radon potential in Abeokuta, Southwest Nigeria. *J Radiat Res Appl Sci.* 2022;15(2):55–8.
- Tchorz-Trzeciakiewicz DE, Rysiukiewicz M. Ambient gamma dose rate as an indicator of geogenic radon potential. *Sci Total Environ.* 2021;755:142771.
- Szegvary T, Leuenberger MC, Conen F. Predicting terrestrial 222 Rn flux using gamma dose rate as a proxy. *Atmos Chem Phys.* 2007;7(11):2789–95.
- BUCREP. La population du Cameroun en 2010 (3e RGPH). Technical Report BUCREP. Yaoundé, 10;2010.
- ONGUENE M, GEORGES P. Différenciations pédologiques dans la région de Yaoundé (Cameroun): transformation d'un sol ferrallitique rouge en sol a horizon jaune et relation avec l'évolution du modèle. 1993.(In French)
- Nzenti JP. Neoproterozoic alkaline meta-igneous rocks from the Pan-African North Equatorial Fold Belt (Yaounde, Cameroon): biotitites and magnetite rich pyroxenites. *J African Earth Sci.* 1998;26(1):37–47.
- Nngotué T, Nzenti JP, Barbey P, Tchoua FM. The Ntui-Betamba high-grade gneisses: a northward extension of the Pan-African Yaoundé gneisses in Cameroon. *J African Earth Sci.* 2000;31(2):369–81.
- Mvondo H, den Brok SWJ, Ondoa JM. Evidence for symmetric extension and exhumation of the Yaounde nappe (Pan-African fold belt, Cameroon). *J African Earth Sci.* 2003;36(3):215–31.

21. Nzenti JP, Barbey P, Macaudiere J, Soba D. Origin and evolution of the late Precambrian high-grade Yaounde gneisses (Cameroon). *Precambrian Res.* 1988;38(2):91–109.
22. Olivry JC. Fleuves et rivières du Cameroun: Monographies hydrologiques Paris: MESRES-ORSTOM; 1986.
23. Takounjou AF, Fantong W, Ngoupayou NJ, Nkamdjou SL. Comparative analysis for estimating hydraulic conductivity values to improve the estimation of groundwater recharge in Yaoundé-Cameroon. *Br J Environ Clim Change.* 2012;2(4):391.
24. Markus 10. Measurements of radon in soil version 1.3. 2011 [cited Sept 5, 2022]. Available from: <https://www.radonmarket.com/Resources/Radonova/Markus10-en-v1.3.pdf>
25. Gammadata. User's guide MARKUS 10 version 1.4: the instrument for determining the radon content in the soil. 1996 [cited Sept. 5, 2022]. Available from: https://www.radon-analytics.com/pdf/Datenblatt_Markus10.pdf
26. Junge CE. *Air Chemistry and Radioactivity.* Int Geophys Ser. New York: Academic Press; 1963.
27. Al-bakhat YMZ, Al-Ani NHK, Mohammed BF, Ameen NH, Jabr ZA, Hammid SH. Measurement of radon activity in soil gas and the geogenic radon potential mapping using RAD7 at Al-Tuwaitha nuclear site and the surrounding areas. *Radiat Sci Technol.* 2017;3(3):29–34.
28. Kumari P, Kumar G, Prasher S, Kumar M, Kumar S, Mehra R, *et al.* Mathematical modelling to estimate radon exhalation rates: a study on soil samples from Pangri valley of Chamba district, Himachal Pradesh, India. *J Phys: Conf Ser.* 2022;2267:012123.
29. Nassiri-Mofakham N, Kakaei M, Alavi M. A study on radon diffusion and exhalation of soils under transient conditions: Theoretical and experimental approach. *Appl Radiat Isot.* 2023;192:110616.
30. Gondji DS, Monempinb JV, Oumar Bobbo M, Tchuenté Siaka YF, Beyala AJF, Saïdou, *et al.* Radon risk assessment and correlation study of indoor radon, radium-226, and radon in soil at the cobalt-nickel bearing area of Lomié, Eastern Cameroon. *Water, Air, Soil Pollut.* 2022;233(6):1–15.
31. SARAD GmbH. Manual NucScout. Portable Gamma Identifier – Quantifier – Dose Rate Meter Version September 2018. Dresden, Germany.
32. Saïdou, Tokonami S, Janik M, Samuel BG, Abdourahimi, Ndjana Nkoulou JE. Radon-thoron discriminative measurements in the high natural radiation areas of Southwestern Cameroon. *J Environ Radioact.* 2015;150:242–6.
33. Pellegrini D. Study of radon emanation from uranium mill tailings. Relations between radon emanating power and physicochemical properties of the material. Fontenay-aux-Roses:CEA;1999.
34. Bajwa BS, Singh H, Singh J, Singh S, Sonikawade RG. Environmental radioactivity: a case study in HHP granitic region of Tusham ring complex Haryana, India. *Geophys Res Abst.* 2010;12:EGU2010–1888.
35. UNSCEAR. UNSCEAR 2000 Report to the General Assembly, with Scientific Annexes. New York, United States: United Nation; 2000.
36. Hosoda M, Sorimachi A, Yasuoka Y, Ishikawa T, Sahoo SK, Furukawa M, *et al.* Simultaneous measurements of radon and thoron exhalation rates and comparison with values calculated by UNSCEAR equation. *J Radiat Res.* 2009;50(4):333–43.
37. Oumar Bobbo M, Tamakuma Y, Suzuki T, Yamada R, Zhuo W, Kranrod C, *et al.* Long-term measurements of radon and thoron exhalation rates from the ground using the vertical distributions of their activity concentrations. *Int J Environ Res. Public Health.* 2021;18(4):1489.
38. Gulan L, Spasović L. Outdoor and indoor ambient dose equivalent rates in Berane town, Montenegro. In RAD5 Proceeding of Fifth International Conference on Radiation and Applications in Various Fields of Research. RAD Association; 2017. p.137–140.
39. Kasić A, Kasumović A. Correlation of the ambient dose equivalent rate and meteorological parameters. *J Radioanal Nucl Chem.* 2020;326(1):147–55.
40. Giustini F, Voltaggio M, Brilli M, Ciotoli G, Ruggiero L, Sirianni P. Determining the outdoor and indoor ambient dose equivalent rates in Celleno municipality (Central Italy). *Geophys Res Abst.* 2019;21:EGU2019–13283.
41. Stojanovska Z, Boev B, Zunic ZS, Ivanova K, Ristova M, Tsenova M, *et al.* Variation of indoor radon concentration and ambient dose equivalent rate in different outdoor and indoor environments. *Radiat Environ Biophys.* 2016;55(2):171–83.
42. Hosoda M, Fukui Y, Pornnumpa C, Sorimachi A, Ishikawa T, Yachi M, *et al.* Absorbed dose rate in air at the Bunkyo-cho campus of Hirosaki University. *Radiat Environ Med.* 2014;3(1):59–62.
43. Saïdou, Oumar Bobbo M, Emmanuel NNIJ, Olga G, Kountchou NM, Hamadou YA. Indoor radon measurements using radon track detectors and electret ionization chambers in the bauxite-bearing areas of Southern Adamawa, Cameroon. *Int J Environ Res Public Health.* 2020;17(18):1–12.
44. Oumar Bobbo M, Saïdou, Ndjana Nkoulou JE, Suzuki T, Kudo H, Hosoda M, *et al.* Occupational natural radiation exposure at the uranium deposit of Kitongo, Cameroon. *Radioisotopes.* 2019;68(9):621–30.
45. Koyang F, Awé R, Bineng GS, Ndimantchi A, Hamadou YA, Saïdou, *et al.* Assessment of natural radiation exposure due to ²²²Rn and external radiation sources: case of the Far North, Cameroon. *Health Phys.* 2022;123(6):444–56.